

Dynamic fluctuations of elastic lines in random environments

SEBASTIAN BUSTINGORRY,¹ JOSÉ LUIS IGUAIN,² CLAUDIO CHAMON,³ LETICIA F. CUGLIANDOLO,^{4,5} AND DANIEL DOMÍNGUEZ¹

¹ *Centro Atómico Bariloche, 8400 San Carlos de Bariloche, Río Negro, Argentina*

² *Departamento de Física, FCEyN, Universidad Nacional de Mar del Plata, Deán Funes 3350, 7600, Mar del Plata, Argentina*

³ *Physics Department, Boston University, 590 Commonwealth Av., Boston MA 02215, USA*

⁴ *Université Pierre et Marie Curie – Paris VI, LPTHE UMR 7589, 4 Place Jussieu, 75252 Paris Cedex 05, France*

⁵ *Laboratoire de Physique Théorique de l'École Normale Supérieure, 24 rue Lhomond, 75231 Paris Cedex 05, France*

PACS. 64.60.Ht – 75.10.Nr.

Abstract. – We study the fluctuations of the two-time dependent global roughness of finite size elastic lines in a quenched random environment. We propose a scaling form for the roughness distribution function that accounts for the two-time, temperature, and size dependence. At high temperature and in the final stationary regime before saturation the fluctuations are as the ones of the Edwards-Wilkinson interface evolving from typical initial conditions. We analyze the variation of the scaling function within the aging regime and with the distance from saturation. We speculate on the relevance of our results to describe the fluctuations of other non-equilibrium systems such as models at criticality.

The study of dynamic fluctuations may serve to grasp the nature of non-equilibrium phenomena. Building upon previous analysis of critical static and dynamic fluctuations [1, 2], Rácz [3] proposed to use the scaling functions characterizing the fluctuations of macroscopic - global - observables in *non-equilibrium steady states* as a classification tool. By introducing ‘universality classes’ in this way, one could then use them to uncover symmetries and dynamic mechanisms in experimental systems.

Another class of non-equilibrium phenomena, including important problems such as glassiness and coarsening, is characterized by a slow relaxation with loss of stationarity [4, 5]. It is by now becoming clear that the study of fluctuations [6] is necessary to understand the mechanism for the slowing down and the *aging non-equilibrium relaxation* in these cases too [7, 8].

An elastic line under the effect of quenched disorder is a relatively simple system with many aspects of glassiness due to the competition between elasticity and disorder. Its physical realizations are manifold, including interfaces in random ferromagnets [9], crack propagation [10], and vortex lines in high- T_c dirty superconductors [11]. The global noise and disorder averaged

displacement and linear response age with a *multiplicative* temporal scaling [12,13] similar to what is found at criticality [14] and in Sinai diffusion [15]. In this Letter we study the line's fluctuating relaxation by analyzing the probability distribution functions (pdfs) of the two-time dependent global roughness and we discuss it in comparison to what has been found in other aging systems [6–8] and the Edwards-Wilkinson (EW) interface [2].

We study a lattice string of length L directed along the y direction of a rectangular square lattice of transverse size $M \gg L^{2/3}$ ($M = 10^4, L = 500$) ensuring the existence of many nearly equivalent ground states. The line segments, x_y ($y = 1, \dots, L$), obey the restricted solid-on-solid (SOS) rule $|x_y - x_{y-1}| = 0, 1$. A quenched random potential V taking independent values on each lattice site is drawn from a uniform distribution in $[-1, 1]$; we use $10^5 - 10^7$ realization depending on L . The initial configuration ($t = 0$) is drawn from the equilibrium distribution at the high $T = 5$. At each microscopic time step we attempt a move of a randomly chosen segment to one of its neighbours restricted by the SOS condition and we accept it with the heat-bath rule. One Monte Carlo (MS) step is defined as L update attempts. In the following we use adimensional time, space and energy scales [12].

The glassy phenomenon appears in this model as a dynamic crossover [12,13]. For all observation times, t_{obs} , that are longer than a size and temperature dependent *equilibration time*, t_{eq} , the dynamics is stationary. Instead, for $t_{obs} < t_{eq}$ the relaxation occurs out of equilibrium as demonstrated by two-time correlations that age. The latter are measured as follows. After equilibration at high T the system is quenched to low T and time is set to zero. The line relaxes until a waiting-time, t_w , when the quantities of interest are recorded and later compared to their values at a subsequent time t .

In this Letter we focus on the *two-time* global roughness

$$w^2(t, t_w) \equiv L^{-1} \sum_{y=1}^L |\delta x_y(t) - \delta x_y(t_w)|^2, \quad (1)$$

with $\delta x_y(t) \equiv x_y(t) - \bar{x}(t)$ the distance from the center of mass, $\bar{x}(t) \equiv L^{-1} \sum_{y=1}^L x_y(t)$. Before any averaging, w^2 fluctuates when changing the disorder and thermal noise realizations.

At high T , neglecting a short transient, the disorder and thermal averaged roughness, $\langle w^2 \rangle$, is stationary and crosses over from growth to saturation at $t_x \sim L^z$ [16]:

$$\langle w^2(t, t_w) \rangle \sim L^\zeta f(\Delta t/t_x), \quad \Delta t \equiv t - t_w, \quad (2)$$

where the scaling function obeys $f(x) \sim x^\beta$ for $x \ll 1$ and $f(x) \sim 1$ for $x \gg 1$, with ζ , β and $z = \zeta/\beta$ the roughness, growth and dynamic exponents, respectively. For the EW line in $1 + 1$ dimensions $\zeta = 1$, $\beta = 1/2$ and $z = 2$. In the presence of disorder, ζ is expected to take a ‘thermal’ value, ζ_{th} , for $L < L_c(T)$, and a larger ‘disorder’ dominated value, ζ_{dis} , for $L > L_c(T)$, both being T -independent [16].

For not too short L and sufficiently low T , t_{eq} goes beyond the numerically accessible time-window and $\langle w^2 \rangle$ depends on t_w explicitly. Before saturation one expects

$$\langle w^2(t, t_w) \rangle \sim \ell^\zeta(t_w) \langle \tilde{w}^2[\ell(t)/\ell(t_w)] \rangle \equiv \ell^\zeta(t_w) \mathcal{F}[\ell(t)/\ell(t_w)] \quad (3)$$

with $\ell(t)$ a growing length (dimensions are restored by prefactors that we omit). This form approaches a stationary regime when $t_w \ll \Delta t \ll t_x$ if $\mathcal{F}(x) \sim x^\zeta$ for $x \gg 1$, and complete saturation at L^ζ when $\ell(t) \rightarrow L$. We found data collapse using $\ell(t) \sim t^{\alpha/\zeta}$ with a *small* exponent [17] and $\mathcal{F}[\ell(t)/\ell(t_w)] = \mathcal{G}(\Delta t/t_w)$ with

$$\mathcal{G}(x) \sim x^\alpha A 10^{Bg(x)} \rightarrow x^\alpha A 10^{\pm B}, \quad (4)$$

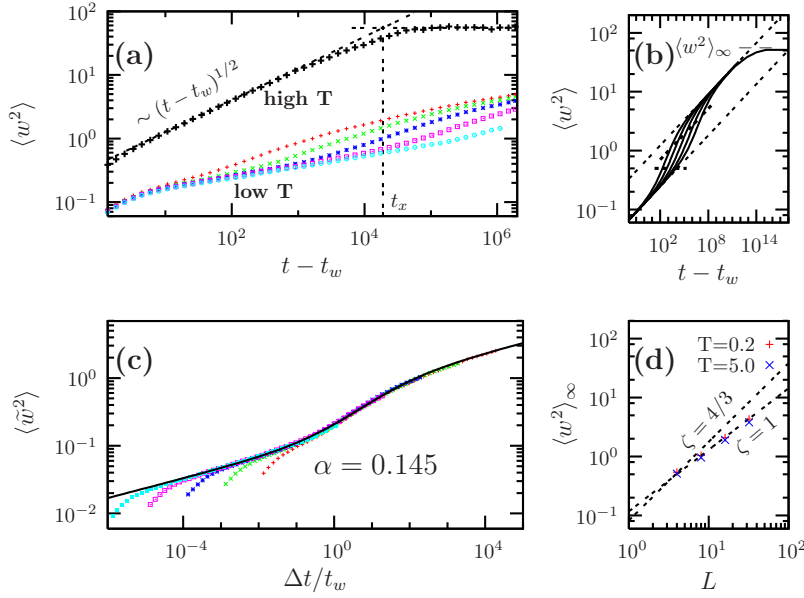


Fig. 1 – (Colour on-line.) Panel (a): thermal and disorder averaged square roughness as a function of time-difference for a line with $L = 500$. The top curve is for $T = 5$; the dotted lines indicate the sub-diffusive regime, saturation and the characteristic time t_x . The high- T dynamics is stationary and conforms with the scaling in (2). The bottom curves are for $T = 0.2$, and $t_w = 10^2, 10^3, 10^4, 10^5, 10^6$ MCs from top to bottom. At low T , stationarity is lost after an initial Δt regime. Saturation is out of the Δt window for all low T curves. Panel (b): sketch of the time-difference dependence of the averaged roughness for several waiting-times. The solid lines have been drawn using the function \mathcal{G} in eq. (4) and a crossover to saturation at $\langle w^2 \rangle_\infty$. The dashed lines represent the asymptotic power laws $c_{1,2}(T)\Delta t^\alpha$. The horizontal dotted line indicates a path of constant $\langle w^2 \rangle / \langle w^2 \rangle_\infty$. The intersection of the curves with the inclined dotted line correspond to constant ν_1 , see eq. (7). Panel (c): scaling of the data in panel (a) using eqs. (3)-(4); the solid line is \mathcal{G} in (4) with $\alpha = 0.145$, $A = 0.28$, $B = 0.35$, $C = 0.56$ and $D = 5.01$. Panel (d): L -dependence of the saturation value, $\langle w^2 \rangle_\infty$, at high and low T .

in the limits $x \gg 1$ and $x \ll 1$, respectively, and $g(x) = \tanh[C \log_{10}(x/D)]$ which does not have a special significance but serves to select the working times Δt and t_w below. Note that on the two asymptotes stationarity is recovered:

$$\langle w^2 \rangle \sim c_{1,2}(T) \Delta t^\alpha, \quad \text{with } \alpha < \beta_{EW} = 0.5, \quad (5)$$

and different proportionality constants $c_{1,2} = A 10^{\mp B}$. α is then a generalization of the growth exponent, β and $\alpha < \beta_{EW}$ reflects that disorder slows down the dynamics. In Fig. 1 we show $\langle w^2 \rangle$ at high and low T : panels (a) and (c) display numerical data and panel (b) presents a sketch of the size and time-dependence of $\langle w^2 \rangle$ at low T . Details are given in the caption.

Even though $\langle w^2 \rangle$ weakly depends on the polymer size before saturation, the saturation value strongly depends on L and it turns out to be important to describe the fluctuations. Transfer matrix calculations show that the static roughness $W_y^2 \equiv \langle [x_y - x_0]^2 \rangle$ with x_0 fixed crosses over from $W_y^2 \sim y$ to $W_y^2 \sim y^{4/3}$ at a length $y^* \sim 5$ at $T = 0.2$ [12]. One might expect a similar crossover for the asymptotic global roughness (1) though the crossover length y^* should not necessarily be the same. With MC simulations we can only determine $\langle w^2 \rangle_\infty \equiv \lim_{\Delta t \gg t_x} \langle w^2 \rangle$ for rather short polymer lengths ($L \leq 32$) both at high and low temperature.

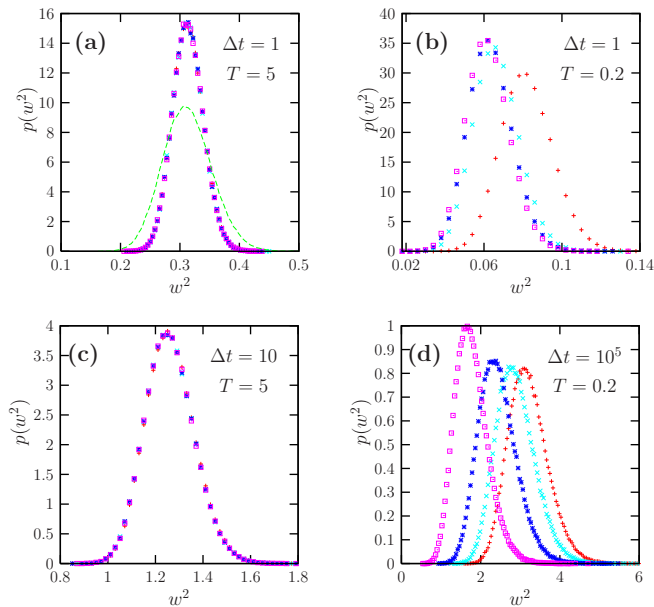


Fig. 2 – (Colour on-line.) Bare square roughness fluctuations at $T = 5$ [(a) and (c)] and $T = 0.2$ [(b) and (d)] for a line with $L = 500$. The time-differences are given in the key. The waiting-times are $t_w = 10^1, 10^2, 10^3, 10^4$ MCs [from right to left in panels (b) and (d)]. In panel (a) one curve (dashed green) for $L = 100$ and the same parameters is included to highlight the L -dependence of the fluctuations.

Figure 1(d) shows its L -dependence at $T = 5$ and $T = 0.2$, two values that we shall use in the rest of the Letter. The dependence is linear with no sign of the crossover to the disorder-dominated regime up to the maximum length, $L = 50$.

We now turn to the study of fluctuations. In Fig. 2 we show the pdf of square roughness fluctuations, $p(w^2)$, for a line with $L = 500$ at $T = 5$ [left, panels (a) and (c)] and $T = 0.2$ [right, panels (b) and (d)] for several values of t_w and Δt given in the keys. At $T = 5$ there is no t_w dependence. The pdfs evolve with Δt and they basically take the EW form [2]. At low T a clear t_w dependence appears at sufficiently (but not too) long Δt 's.

In order to understand $p(w^2)$ we propose a scaling form that we later put to the test numerically. In the low T regime, for times such that equilibration has not been reached ($t_w \ll t_{eq}$) $p(w^2)$ depends on the (already adimensional) times t and t_w , the system size L and temperature T . With a simple change of variables we measure w^2 in units of its average $\langle w^2 \rangle$: $p(w^2; t, t_w, L, T) = \langle w^2 \rangle^{-1} \rho(w^2 / \langle w^2 \rangle; t, t_w, L, T)$. Using eq. (3), and the monotonicity of ℓ and \mathcal{G} , the dependence on t and t_w can be replaced by a dependence on $\langle w^2 \rangle$ and $\langle \tilde{w}^2 \rangle$. L can be traded for the T -dependent saturation value $\langle w^2 \rangle_\infty$. Now, our *scaling hypothesis* is that the dependence on $\langle w^2 \rangle$ occurs only in comparison with the saturation value:

$$\langle w^2 \rangle p(w^2) = \bar{\Phi} \left(w^2 / \langle w^2 \rangle; \langle \tilde{w}^2 \rangle, \langle w^2 \rangle / \langle w^2 \rangle_\infty, T \right). \quad (6)$$

This form holds exactly at high temperatures and for the EW interface. In these cases disorder is irrelevant or even absent and the t_w -dependence, and hence the $\langle \tilde{w}^2 \rangle$ -dependence, disappears. In addition, all T dependence enters through $\langle w^2 \rangle_\infty$ and one has $\langle w^2 \rangle p(w^2) = \Phi_{EW}(w^2 / \langle w^2 \rangle, \langle w^2 \rangle / \langle w^2 \rangle_\infty)$ [2].

To account for the $\langle \tilde{w}^2 \rangle$ dependence we introduce the parameter

$$\nu_1 \equiv [\langle \tilde{w}^2 \rangle - c_1(\Delta t/t_w)^\alpha]/[(c_2 - c_1)(\Delta t/t_w)^\alpha] \quad (7)$$

within the description of the averaged data with the power fit $\ell(t) \sim t^{\alpha/\zeta}$. ν_1 varies between 0 and 1 when $\langle \tilde{w}^2 \rangle$ moves from the first to the second asymptotic power laws before saturation, see the dashed lines in Fig. 1(b) and eq. (5). We call $\nu_2 \equiv \langle w^2 \rangle / \langle w^2 \rangle_\infty$ the second parameter in (6). Then, by choosing groups of $(L, \Delta t, t_w)$ we vary ν_1 and ν_2 . In the following we test the following restatement of our scaling hypothesis

$$\langle w^2 \rangle p(w^2) = \Phi(w^2 / \langle w^2 \rangle; \nu_1, \nu_2, T) . \quad (8)$$

In Fig. 3(a) we plot data for $\nu_1 = 0.389$ and different ν_2 . We use $\langle w^2 \rangle_\infty \sim L$ and we plot six sets of data corresponding to two values of $\nu_2 = \langle w^2 \rangle / L$ (the T -dependent prefactor is irrelevant since we are working at constant T). The two sets of data with the same ν_2 collapse rather well. The dependence on ν_2 is similar to the one found for the EW line: for small ν_2 the scaling function has an approximately log-normal form, it is positively skewed and it gets wider with increasing ν_2 . In panel (b) we use instead $\langle w^2 \rangle_\infty \sim L^{4/3}$ and the scaling variable $\nu_2 = \langle w^2 \rangle / L^{4/3}$. The collapse is now lost in accordance with our hypothesis and the fact that $\langle w^2 \rangle_\infty \sim L$ for the lengths used. (It would of course be desirable to have an independent determination of $\langle w^2 \rangle_\infty$ to confirm our conclusions.)

In Fig. 3(c) we analyze the evolution of Φ with ν_1 . Φ resembles the high T result with the same distance from saturation (black solid line) when $\nu_1 \rightarrow 1$ and $\langle w^2 \rangle \sim c_2(T)\Delta t^\alpha$. It progressively deviates from the high T form for decreasing ν_1 . Decreasing ν_1 while keeping ν_2 fixed has a similar effect as increasing ν_2 while keeping ν_1 fixed: Φ gets closer to the asymptotic disorder-free form, $\lim_{\Delta t \gg t_x} \Phi_{EW}$. Moreover, at fixed and small ν_2 the ν_1 -dependent pdfs can also be quite well described with a log-normal function with two ν_1 -dependent parameters.

The ν_1 dependence can be rationalised from the point of view of the dynamics in a free-energy landscape. For each t_w there is a sufficiently long Δt such that $\langle w^2 \rangle \sim c_2(T)\Delta t^\alpha$ and the waiting-time dependence disappears (see Fig. 1). After these very long Δt 's one allows the system to get out of the traps occupied at t_w , sub-diffuse with $\alpha < \beta_{EW} = \frac{1}{2}$ but fluctuate similarly to the high T and Gaussian cases once the good scaling variables are chosen, as shown by the fact that $p(w^2)$ gets very close to the continuous curve in Fig. 3(c). In the opposite limit in which $\langle w^2 \rangle$ has not deviated much from the first asymptote the system is quite trapped and has not had enough time-difference, Δt , to explore a relevant part of the free-energy landscape. The fluctuations are then very different from the high- T and disorder-free ones.

In the inset to Fig. 3(a) we show data from the Langevin dynamics of a *continuous* model of an elastic line in a $3d$ disordered environment [13, 20] that confirms the scaling form and the generic trend. We shall present more details on the functional form of Φ in the lattice and continuous models as well as on the T -dependence in a longer publication [23].

Summarizing, we studied the effect of disorder on the low- T averaged and fluctuating two-time roughness of elastic lines. On the one hand disorder introduces aging at sufficiently low temperatures. Thus, a time-delay that increases with the waiting-time is necessary to enter a stationary regime next to saturation. On the other hand, it slows down the evolution and the averaged roughness in this last dynamic regime undergoes sub-diffusion with a smaller exponent than in the EW case. Well before saturation the two-time roughness fluctuations can be represented by a scaling function, Φ , that depends on where in the aging regime the dynamics take place (parametrized by $\langle \tilde{w}^2 \rangle$ or ν_1) and the distance from saturation (given by $\nu_2 \equiv \langle w^2 \rangle / \langle w^2 \rangle_\infty$). At high T , and at low T but close to the sub-diffusive regime before saturation, disorder is quite irrelevant and Φ approaches the EW form Φ_{EW} depending only

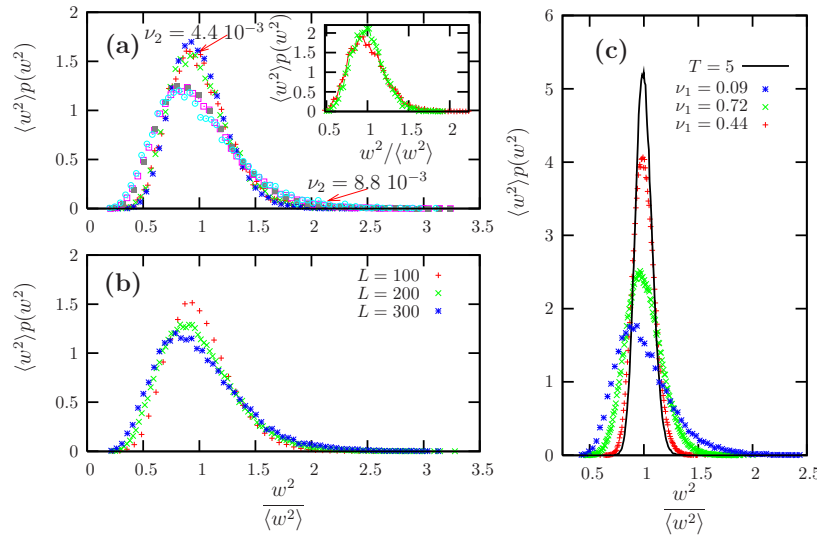


Fig. 3 – (Colour on-line.) Panel (a): check of the scaling (6) using $\langle w^2 \rangle_\infty \propto L$ ($\zeta = 1$). The gray filled squares ($L = 100$, $t_w = 100$), pink open squares ($L = 200$, $t_w = 1.19 \cdot 10^4$) and cyan open circles ($L = 300$, $t_w = 1.95 \cdot 10^5$) data are at the same distance from saturation ($\nu_2 = \langle w^2 \rangle / L = 8.8 \cdot 10^{-3}$), and have the same ‘aging’ roughness ($\nu_1 = 0.389$, $\Delta t / t_w = 10$). The blue \star ($L = 200$, $t_w = 10^2$), green \times ($L = 400$, $t_w = 1.19 \cdot 10^2$) and red $+$ ($L = 600$, $t_w = 1.95 \cdot 10^5$) data are for $\nu_2 = 4.4 \cdot 10^{-3}$ and the same ν_1 as the other group. Inset: the pdf for the continuous model in [13]. Panel (b): test of the scaling (6) using $\langle w^2 \rangle_\infty \propto L^{4/3}$ ($\zeta = 4/3$) and $\nu_2 = \langle w^2 \rangle / L^{4/3} = 1.3 \cdot 10^{-3}$. Panel (c): Dependence on ν_1 and comparison with the high- T behaviour (black solid line). One gets deeper into the aging regime in the order blue \star ($\Delta t = 2.25 \cdot 10^5$, $t_w = 10^6$, $\nu_1 = 0.09$), green \times ($\Delta t = 1.50 \cdot 10^3$, $t_w = 10^2$, $\nu_1 = 0.44$), red $+$ ($\Delta t = 1.50 \cdot 10^2$, $t_w = 10^0$, $\nu_1 = 0.72$). $\nu_2 = \langle w^2 \rangle / L = 2 \cdot 10^{-3}$.

on ν_2 . At intermediate time-scales, where the waiting-time dependence is explicit, Φ deviates from the free result and becomes broader and less symmetric. The dependence on the distance to saturation at fixed ‘aging’ parameter ν_1 is similar to the one in the EW line.

We conjecture that this kind of scaling appears also in line problems in different universality classes, *e.g.* KPZ [21], and/or for other quantities such as the maximum height with respect to the mean [22]. It would also be interesting to study these features in the out of equilibrium dynamics of critical systems [14] and random walkers in random environments [15] with a multiplicative scaling of two-time correlations and responses.

This study extends the proposal in [7] for the fluctuations in aging systems with additive scaling – correlations that approach a well-defined and finite plateau to later further decay to zero – to problems with *diffusive aging* and a strong dependence on the system size. In the former cases one could explain the scaling and generic form of the pdfs as a consequence of the emergence of a symmetry, *time reparametrization invariance*, in the long time dynamics. The presence of the symmetry allowed one to propose an effective action for the most important fluctuations, and derive from it the pdfs of local correlations and responses that have been partially confronted to experimental measurements in colloidal suspensions [6] and simulations of kinetically constrained models and finite dimensional spin-glass models [7]. The study of the symmetry properties of the long-times dynamics of elastic lines in random environments and further identification of an effective sigma-model-type action for the fluctuations remains

to be done. It should be possible to use it to compute (6).

We acknowledge useful discussions with A. Kolton and H. Yoshino and financial support from SECYT-ECOS P. A01E01 (LFC, DD), CNEA, CONICET PIP05-5596 (SB, DD) and PIP05-5648 (JLI), ICTP-NET-61 (DD, JLI), ANPCYT PICT04-20075 (JLI), Fundación Antorchas (SB), NSF-CNRS INT-0128922 (CC, LFC), PICS 3172 (LFC), and NSF DMR-0305482 and DMR-0403997 (CC). SB and LFC thank the UNMDP for hospitality. JLI is indebted to the Réseau Québécois de Calcul de Haute Performance for generous allocations of computer resources. LFC is a member of IUF.

REFERENCES

- [1] G. Foltin *et al*, Phys. Rev. E **50**, R639 (1994). M. Plischke *et al*, Phys. Rev. E **50**, 3589 (1994). Z. Rácz and M. Plischke, Phys. Rev. E **50**, 3530 (1994). S. T. Bramwell *et al*. Nature **396**, 552 (1998).
- [2] T. Antal and Z. Racz, Phys. Rev. E **54**, 2256 (1996).
- [3] Z. Rácz, SPIE proceedings Vol. 5112, 248 (2003).
- [4] E. Vincent, J. Hammann, M. Ocio, J-P Bouchaud, and L. F. Cugliandolo, in *Complex behaviour in glassy systems* E. Rubi ed. (Springer-Verlag, 1997), cond-mat/9607224.
- [5] L. F. Cugliandolo in *Slow Relaxations and Nonequilibrium Dynamics in Condensed Matter*, J. -L. Barrat *et al*. Eds., (Springer, Berlin, 2002).
- [6] R. Courtland, and E. Weeks, J. Phys. C **15**, S359 (2003). K. S. Sinnathamby, H. Oukris, and N. E. Israeloff, cond-mat/0412378. L. Cipelletti and L. Ramos, J. Phys. C **17**, R253 (2005). A. Duri, H. Bissig, V. Trappe, and L. Cipelletti, Phys. Rev. E **72**, 051401 (2005). P. Wang, C. Song, and H. Makse, Nature Physics **2**, 526 (2006).
- [7] C. Chamon, M. P. Kennett, H. Castillo, and L. F. Cugliandolo, Phys. Rev. Lett. **89**, 217201 (2002). H. E. Castillo, C. Chamon, L. F. Cugliandolo, and M. P. Kennett, Phys. Rev. Lett. **88**, 237201 (2002); H. E. Castillo, C. Chamon, L. F. Cugliandolo, J. L. Iguain, and M. P. Kennett, Phys. Rev. B **68**, 134442 (2003). C. Chamon, P. Charbonneau, L. F. Cugliandolo, D. Reichman, and M. Sellitto, J. Chem. Phys. **121**, 10120 (2004).
- [8] C. Chamon, L. F. Cugliandolo, and H. Yoshino, J. Stat. Mech (2006) P01006.
- [9] D. A. Huse and C. L. Henley, Phys. Rev. Lett. **54**, 2708 (1985).
- [10] A. Hansen and E. L. Hinrichsen, and S. Roux, Phys. Rev. Lett. **66**, 2476 (1991).
- [11] See, *e.g.* G. Blatter, M. V. Feigel'man, V. B. Geshkenbein, A. I. Larkin, and V. M. Vinokur, Rev. Mod. Phys. **66**, 1125 (1994); T. Nattermann and S. Scheidl, Adv. in Phys. **49**, 607 (2000).
- [12] H. Yoshino, J. Phys. A **29**, 1421 (1996); Phys. Rev. Lett. **81**, 1493 (1998); and unpublished. A. Barrat, Phys. Rev. E **55**, 5651 (1997).
- [13] S. Bustingorry, L. F. Cugliandolo, and D. Domínguez, Phys. Rev. Lett. **96**, 027001 (2006).
- [14] A. Gambassi and P. Calabrese, J. Phys. A **38**, R133 (2005) and references therein.
- [15] L. Laloux and P. Le Doussal, Phys. Rev. E **57**, 6296 (1998). P. Le Doussal, C. Monthus, and D. S. Fisher Phys. Rev. E **59**, 4795 (1999).
- [16] A-L Barabási and H. E. Stanley, *Fractal concepts in surface growth* (Cambridge University Press, Cambridge, 1995). T. Halpin-Healey and Y-C Zhang, Phys. Rep. **254**, 215 (1995).
- [17] Simulations of a similar model [18] suggest that ℓ crosses over from power-law to logarithmic growth; it is very hard to distinguish a logarithmic growth from a power law with a small exponent as the one we use here. Note that (3) has a $\Delta t \ll t_w$ stationary regime only if $\ell(t) \sim t^a$.
- [18] A. Kolton, A. Rosso, and T. Giamarchi, Phys. Rev. Lett. **95**, 180604 (2005).
- [19] D. R. Nelson and H. S. Seung, Phys. Rev. B **39**, 9153 (1989).
- [20] C. Reichhardt, A. van Otterlo, and G. T. Zimanyi, Phys. Rev. Lett. **84**, 1994 (2000).
- [21] F. D. A. Aarão Reis, cond-mat/0508238.
- [22] S. Majumdar and A. Comtet, Phys. Rev. Lett. **92**, 225501 (2004).
- [23] S. Bustingorry *et al*, in preparation.